Published in final edited form as:
Arch Ophthalmol. 2010 August ; 128(8): 1014–1021. doi:10.1001/archophthalmol.2010.158.

Association of retinal vascular endothelial growth factor with avascular retina in a rat model of retinopathy of prematurity

Steven J. Budd, MS, **Hilary Thompson, PhD**, and **M. Elizabeth Hartnett, MD**
University of North Carolina, Department of Ophthalmology, Chapel Hill, NC 27599-7040, Louisiana State University, School of Public Health, New Orleans, LA

Abstract

Objective—To determine the effect of oxygen fluctuations on the expression of vascular endothelial growth factor (VEGF) and VEGF receptor 1(R1) and VEGFR2 using a rat model of retinopathy of prematurity (ROP).

Methods—Retinas isolated from the ROP model and from room air-raised rat pups (RA) at several post-natal day ages (p) were analyzed for mRNAs of VEGF splice variants, VEGFR1 and VEGFR2 by real-time polymerase chain reaction (PCR). VEGF protein was measured by ELISA.

Results—Older developmental age was associated with increased expression of VEGFR1 and $VEGF_{120}$ mRNAs ($P<.0001$ and $P=.0006$, respectively). VEGFR2 and $VEGF_{164}$ mRNAs were associated with older developmental age ($P<.0001$) or exposure to the ROP model ($P=.0247$ and $P<.0001$, respectively). $VEGF_{120}$ and $VEGF_{164}$ had greater mRNA expression at p14 when 30% avascular retina existed in the ROP model compared to RA in which no avascular retina existed, and at p18 when intravitreous neovascularization existed in the model but not in RA. VEGF protein was significantly increased at p14 and at p18 ($P<.0001$).

Conclusions—Unlike models of oxygen-induced retinopathy that describe ROP prior to implementation of oxygen regulation, the ROP model recreates oxygen stresses relevant to preterm infants with severe ROP today. $VEGF_{164}$ and VEGFR2 mRNA expression and VEGF protein were increased in association with the ROP model and older developmental age and at time points when not only intravitreous neovascularization, but also avascular retina, were present in the ROP model and not in RA, suggesting a role for VEGF regulation in the development of these features.

Introduction

Retinopathy of prematurity (ROP), described in the 1940's[1], was attributed to high oxygen at birth that caused newly developed retinal capillaries to constrict and recess leaving areas of avascular retina[2,3]. When a preterm infant was moved from an oxygen environment to room air, the avascular retina became hypoxic and was thought to be the source of angiogenic factors that caused intravitreous neovascularization (IVNV). This hypothesis[2,4,3] was developed through experimentation with newborn animals exposed to constant, high oxygen followed by room air exposure and provided the basis for several oxygen-induced retinopathy (OIR) models still used today. Smith et al. developed a widely used mouse OIR model, which many investigators have used to determine mechanisms of oxygen stress and relative hypoxia-induced angiogenesis with genetically modified animals[5]. The model has also been used to reflect a transition from *in utero* with low oxygen and maternally-derived factors to sometime after birth when oxygen levels were higher[6], and growth factors,

Corresponding author (and for reprints): M. Elizabeth Hartnett, MD, Department of Ophthalmology, University of North Carolina, 130 Mason Farm Road, CB # Chapel Hill, NC, 27599-7040, Phone (919)-843-0298, FAX (919)-966-1908, hartnet@med.unc.edu.

inadequately produced by the infant, were no longer supplied from the placental circulation[7]. Also, using the model, Smith proposed a biphasic scenario for severe ROP, in which initially there was a “vaso-obliterative phase” (seen as hyperoxia-induced central avascular retina in the mouse OIR model) followed by a “vaso-proliferative phase” (seen as endothelial budding into the vitreous at the junctions of avascular and vascular retina).

For the most part, the mouse OIR model represents ROP in preterm infants exposed to high, unregulated oxygen levels (such as seen in the 1940's in the US) or to infants with delayed retinal vascular development, low growth factor levels[8] and poor postnatal growth[9]. However, the mouse model may not represent most cases of severe ROP that occur in the US today. First, since the initial description of ROP and recognition that high oxygen at birth played a role, technology has developed and been implemented to regulate and monitor oxygen in preterm infants. Now, preterm infants are no longer resuscitated in high oxygen[6] and oxygen saturations are carefully monitored to keep them in the mid 80 to low 90 percentages, depending on the post-gestational age of the infant (these saturations translate to arterial concentrations under 70 mm Hg). In oxygen-induced retinopathy models, including the mouse model, 75% inspired oxygen is used to induce capillary recession and constriction, and this level of inspired oxygen causes arterial oxygen levels higher than 300 mmHg[10]. Second, in most OIR models, constant oxygen, rather than fluctuations in oxygen, is used. However, oxygen levels in the preterm human infant fluctuate on a minute-to-minute frequency even when inspired oxygen is relatively constant, and the extremes of oxygen levels as well as the range of the fluctuations may play a role in human ROP[11]. Third, in the human infant, retinal vascular development to the ora serrata is complete at term, but preterm infants have incomplete vascularization of the retina at birth. With today's ROP, there appears to be a delay in vascularization of avascular retina with areas of peripheral avascular retina and not central “vaso-obliteration” that is a main feature in the mouse OIR model.

Molecular analyses of retinas of the mouse OIR model have reported reduced expression of several growth factors during the “vaso-obliterative phase” of avascular retina[12,13]. Particularly notable is vascular endothelial growth factor (VEGF), an important factor in retinal vascular development[14,15,16] and in pathologic angiogenesis[17]. When VEGF or other factors, including erythropoietin, insulin-like growth factor-1 (IGF-1), or placental growth factor, were injected into the vitreous of an eye in the mouse OIR model prior to hyperoxia, central retinal avascularity was reduced. During the proliferative phase, expression of VEGF, erythropoietin or IGF-1 was increased in association with intravitreous endothelial budding, and inhibition of growth factor bioactivity by several methods led to reduced endothelial budding[18,19,20,21]. In the OIR model, the time period between the two events is within 10 days, whereas in preterm infants severe ROP develops approximately 2 months or more following birth. It is unknown what happens to the retinal growth factor concentration in the human infant during this interval.

To explore the effect of relevant oxygen stresses on the regulation of VEGF splice variants and receptors in association with important features of severe ROP seen today in the US, we used a relevant model, which exposes pups to oxygen levels that produce arterial oxygen concentrations similar to transcutaneous oxygen levels reported in infants with severe ROP in current day[22]. The model also produces a characteristic appearance of severe ROP with peripheral avascular retina similar to zone II ROP[22,23], followed by retinal tortuosity similar to plus disease[24], and then intravitreous neovascularization (IVNV) at the junctions of vascular and avascular retina, similar to stage 3 ROP[25,23]. The model uses fluctuations in oxygen, a risk factor for severe ROP[11]. We measured retinal VEGF protein and the expression of VEGF splice variant and receptor mRNAs in the model and in room air at the same developmental ages.

Methods

All animal studies complied with the University of North Carolina's Institute for Laboratory Animal Research (Guide for the Care and Use of Laboratory Animals) and the ARVO Statement for the Use of Animals in Ophthalmic and Visual Research.

ROP Model

Within 4 hours of birth at postnatal day 0 (p0), litters of 12-14 newborn Sprague-Dawley rat pups with their mothers (Charles River, Wilmington, MA) were placed into an Oxycycler incubator (Biospherix, New York, NY) to cycle inspired oxygen between 50% oxygen and 10% oxygen every 24 hours. Pups from other litters were used to supplement deficient litters. After 7 cycles of oxygen fluctuations at day 14, pups were then placed into room air for 4 days[10]. Oxygen levels were monitored daily and recalibrated as needed. Carbon dioxide in the cage was also monitored daily and was flushed from the system by maintaining sufficient gas-flow and by adding soda lime, if needed.

Dissection of Retinal Tissue for Flat Mounting and mRNA and Protein Analyses

For time point measurements, animals were euthanized with pentobarbital (80 mg/kg intraperitoneal injection) at the time of change in inspired oxygen level. Therefore, pups euthanized at the start of even numbered days up to day 14 had just been exposed to 10% oxygen and odd numbered days, to 50% oxygen. Pups euthanized at day 18 had been exposed to 7 cycles of oxygen fluctuations followed by 4 days in room air. (As an example, a postnatal day 8 pup was starting the 8^{th} day of life and had just been exposed to 10% oxygen.) For flat mounts, eyes were fixed in 2% paraformaldehyde (PFA) for 2 hours. Retinas were isolated[26] with ora serratas intact and placed into phosphate buffered saline (PBS) after the hyaloidal vessels and remaining vitreous were removed. By making 4 incisions 90 degrees apart, the retinas were flattened and then placed onto microscope slides. For fresh tissue, eyes were not fixed in PFA and retinas were dissected without ora serratas. Tissue was frozen in modified radioimmunoprecipitation assay (RIPA) buffer (20 mM Tris base, 120 mM sodium chloride (NaCl), 1% Triton X-100, 0.5% sodium deoxycholate, 0.1% sodium dodecyl sulfate (SDS), 10% glycerol) with a Protease inhibitor cocktail (1:100, Sigma, MO) and 1M orthovanadate (1:100, Sigma, MO), then stored at -20°C for protein or RNAlater (Applied Biosystems, CA) for RNA until analysis.

Tissue Staining and Analysis of Flat Mounts

To stain the vasculature, the flattened retinas were first permeabilized in ice cold 70% v/v ethanol for 20 minutes, then in PBS/1% Triton x-100 for 30 minutes, and then incubated with Alexa Fluor 568 conjugated *G. simplicifolia* (Bandeiraea) isolectin B4 (5 μg/ml, Molecular Probes, OR) in PBS overnight at 4°C, as previously described[27]. Images of the retinal blood vessels were captured using a Nikon 80i Research Upright Microscope with Surveyor/Turboscan software and digitally stored for analysis.

Total retinal area, summed peripheral avascular retinal area and areas of IVNV were computed in pixels with Image Tool v.3 (University of Texas, San Antonio, TX) and converted to mm^2 (using a calibration bar on each image). IVNV was defined as neovascularization growing into the vitreous at the junction of vascular and avascular retina[23]. For clock hours, flat mounts were divided into 12 clock hours of approximately equal area using Adobe Photoshop, assessed for the presence of IVNV[28,29], and assigned a number (0 to 12) depending on the number of clock hours exhibiting IVNV. Areas were measured, summed, and expressed as a percent of total retinal area for each eye. Measurements were performed by two independent masked reviewers. When discrepancies in measurements occurred, these were reviewed and a final consensus determined.

Real-time PCR

Samples were removed from RNAlater and total RNA was extracted using the RNeasy Mini kit (Qiagen, Valencia, CA). DNA contamination was removed by using DNA-free (Ambion, Austin,TX), and RNA quantity was determined spectrophotometrically. 1 μ g of RNA from each sample was reverse transcribed using the High Capacity cDNA Reverse Transcription Kit (Applied Biosystems, Foster City, CA). Approximately 200 ng of cDNA were analyzed per well by one step real time PCR using the TaqMan MasterMix with reverse transcriptase (3.7 U/reaction, Applied Biosystems, Foster City, CA). Primers were specific for rat (annealing temperature 60°C): $VEGF_{164}$: forward 5′GCACATAGGAGAGATGAGCT 3′, probe 5′GCTCACAGTGATTTT CTGGC3′, reverse TGCAG CATAGCAGATGTGAATGCAGACC, $VEGF_{120}$: forward 5′GCACATAGGAGA G ATGAGCT 3′, probe 5′GGCTTGTCACATTTTTCTGGC3′, reverse TGCAGCATAGCAGATGTGA ATGCAGACC, $VEGF_{188}$: forward, 5′CAGTTCGAGGAAAGGGAAAG 3′, probe, 5′CAGTGAACGCTCCAGGATTT3′, reverse ACCGGGATTTC TTGCGCTTTCGTTTTTTG, VEGFR1: forward, 5′CCACCTCCATGTTTGAAGAC3′, probe, 5′AGTCCAGGTGAATC GCTTCA3′, reverse TACCAGCAGTCTGCTGACCTCCCC, VEGFR2: forward 5′CTCCATCTTTTGGTGGGATG3′, probe 5′GCTGGTCTGGTTGGAGCCT3′, reverse AGGCCACAGACTCCCTGCTT TTACTG3, and were made by UNC's Oligonucleotide Core facility (http://www.med.unc.edu/olioli/index.htm). cDNA was mixed 1:1 with Taqman Universal Master Mix (Applied Biosystems, CA) and primers. Rat β-actin was used as a control gene because its expression had been found to be stable under various oxygen stresses previously. Primers for rat β-actin were, forward, TGCCTGACGGTCAGGTCA, probe CACTATCGGCAATGAGCGGTTCCG, and reverse CAGGAAGGAAGGCTGGAAG. Duplicate reactions with a total volume of 16 μL were run for each sample and control using the AB 7500 PCR System. The 7500 System Software calculates cycle threshold (Ct) automatically for each well and each value was normalized to β-actin. DDCt values were then calculated. The p0 time point was within 4 hours of birth and was therefore the same time point for samples from room air pups and those in the ROP model. $VEGF_{188}$ at p0 was assigned a value of 1.0. The values for the three VEGF splice variants in the ROP model and room air were related to this value and graphically represented (Figures 4 – 6). VEGFR1 room air at p0 was scaled to the value of 1.0 for comparisons of time points for room air and the 50/10 OIR model for VEGFR1 (Figure 2). The VEGFR2 value at p0 was 59.6 fold greater than VEGFR1. VEGFR2 room air at p0 was scaled to the value of 1.0 for comparisons of time points for room air and the 50/10 OIR model for VEGFR2 (Figure 3). For statistical analysis, raw data were used.

Protein Analysis

VEGF protein was analyzed with an enzyme-linked immunosorbent assay (ELISA), which measures all VEGF splice variants. The most prevalent splice variants represent the greatest percentage in the ELISA value. Retinal samples frozen in RIPA buffer were thawed, homogenized and centrifuged (16,000×g, 10 minutes, 4°C). Total protein was quantified with a bicinchoninic acid (BCA) protein assay kit (Bio-Rad, Hercules, CA, modified from the Lowry assay[30]). Supernatants were assayed without dilution in duplicate using commercially available ELISA kits, raised against rat VEGF (R& D systems, MN). The mean minimum detectable dose was 6.4 pg/mL for VEGF.

Analysis

In order to maintain the reproducibility of the ROP model, litters were never depleted below 12 pups. Often this required that whole litters be used for individual time points. For each time point, at least 5 retinas from different pups were analyzed from at least two different litters. Graphically represented are the mean fold changes relative to β-actin with error bars

representing standard errors. While these normalized ratios were used for graphical representation in the figures, in order to avoid bias, the raw data were rescaled and statistically analyzed as described below.

Initially, β-actin was analyzed by regression analysis of the ratio of each β-actin/VEGF splice variant or receptor mRNA for the Ct1 value against respective β-actin/VEGF splice variant or receptor mRNA for the Ct2 value, and the slope was found to be indistinguishable from 1.0, which is the ideal value[31]. The geometric means of the product of the two ratios were then determined for each time point and treatment, and this was the outcome analyzed. For the analysis of VEGF protein by ELISA, the protein concentration was the outcome analyzed. A factorial analysis of variance (ANOVA) with a completely randomized treatment arrangement was used to determine the significance of the factors, time point and treatment (room air vs. ROP model) as well as the interaction of time point and treatment. *Post-hoc* testing of treatment and time point by treatment interaction means was accomplished using protected t tests on least squares means, with alpha level adjustment for multiple comparisons among means accomplished using a method of simulation[32].

Results

Retinal Flat Mounts

In p14 room air-raised pups, retinal vascularization of the inner capillary plexus had extended to the ora serrata (Figure1a). There was no avascular retina or IVNV at p14 or p18 in room air. In the ROP model, avascular retina was approximately 30% of the total retinal area at p14, and 25% at p18. No clock hours of IVNV were found at p14 and a median of 7.0 clock hours (3.2± 0.3 mm^2 mean avascular area ± standard error) was present at p18 (Figure 1b). These findings are comparable to those reported in the literature[33].

mRNAs of VEGF Receptors and VEGF Splice Variants

We chose time points to determine expression levels preceding and including postnatal day (p)14 when avascular retina was present in the ROP model, but absent in room air raised pups. We also analyzed p18 for IVNV. A previous study has reported on VEGF protein concentration at time points following p14 and preceding the development of IVNV in the ROP model[29].

VEGFR1 mRNA increased many fold during development (Figure 2). For example, from p0 to p14, VEGFR1 mRNA increased 42 fold and from p0 to p18, 75 fold. By statistical analysis, increased fold expression of VEGFR1 was significantly associated with older developmental age ($P<.0001$), but not with whether pups had been placed into the ROP model or room air. In contrast, the fold increase in VEGFR2 mRNA was relatively less than for VEGFR1 mRNA. For example, from p0 to p14, VEGFR2 mRNA increased approximately 5 fold and from p0 to p18, approximately 3 fold (Figure 3). Furthermore, there was a significant increase in expression associated with older developmental age ($P<.0001$) and with exposure to the ROP model compared to room air ($P=.0247$).

We previously reported that $VEGF_{164}$ was the most prevalent and $VEGF_{188}$ the least prevalent splice variant in the ROP model using relative quantitative RT-PCR[33]. Using real time PCR, we confirmed these findings. Since VEGF expression was reduced during the "vaso-obliterative" phase in the mouse OIR model, we predicted that the most prevalent VEGF splice variant, $VEGF_{164}$, would have lower fold expressions in the ROP model at the developmental age when avascular retina existed in the ROP model compared to room air when no avascular retina was present. However, the fold expression in $VEGF_{164}$ mRNA was greater in the ROP model than in room air at p14. By statistical analysis of $VEGF_{164}$, there was a significant increase in expression associated with older developmental age ($P<$.

0001) and with exposure to the ROP model compared to room air ($P<.0001$). Since VEGF is upregulated in hypoxia and downregulated in hyperoxia[34], we anticipated that the pattern of $VEGF_{164}$ expression would show a greater fold expression following 24 hours in hypoxia (p12 and p14) and a lower fold expression following 24 hours in hyperoxia (p11 and p13). As predicted, the pattern of $VEGF_{164}$ expression varied based on whether hypoxia or hyperoxia had occurred in the ROP model (Figure 4). In agreement with our predictions, at p18 when IVNV was present in the ROP model, the $VEGF_{164}$ expression was greater in the ROP model than in room air. For $VEGF_{120}$, the pattern of upregulation following hypoxia and downregulation following hyperoxia was also noted (Figure 5). However, by statistical analysis, only older developmental age was significantly associated with increased expression of $VEGF_{120}$ ($P=.0006$). There was no significant association with exposure to the ROP model compared to room air ($P=.61$). $VEGF_{188}$ had greater fold expression at most time points in room air compared to the ROP model, but there was no significant association with developmental age or with exposure to the ROP model compared to room air (Figure 6).

VEGF Protein Concentration in Room Air and ROP Model—VEGF protein was significantly associated with older developmental age or with exposure to the ROP model compared to room air (both $P<.0001$). VEGF protein shared some similarities in the pattern of expression as fold changes in $VEGF_{164}$ mRNA (Figure 7). By *Post-hoc* testing, there was significant increases in VEGF protein in the ROP model compared to room air at both p14 and p18 ($P<.0001$).

Discussion

We analyzed retinal mRNA expression of VEGF splice variants, VEGFR1 and VEGFR2, and of VEGF protein at different developmental time points in room air and in a rat ROP model that uses oxygen extremes and fluctuations relevant to human preterm infants, who develop severe ROP today. This model also has a retinal appearance similar to human zone II, stage 3 ROP. We found that increased expression of $VEGF_{164}$ was significantly associated with older developmental age or exposure to the ROP model compared to room air, whereas increased expression of $VEGF_{120}$ was significantly associated with older developmental age and not with exposure to the ROP model. The fold changes of the least prevalent splice variant, $VEGF_{188}$, were not significantly affected by developmental age or exposure to the ROP model compared to room air. VEGFR1 expression was significantly increased in association with older developmental age, but not with exposure to the ROP model, whereas VEGFR2 expression was significantly increased in association with older developmental age or with exposure to the ROP model.

We previously reported that $VEGF_{164}$ expression, measured with relative quantitative RT-PCR, was increased after repeated fluctuations in oxygen but not after a single episode of 10% oxygen exposure, whereas $VEGF_{120}$ was upregulated following an episode of hypoxia and not after repeated fluctuations in oxygen [33]. As fluctuations in transcutaneous oxygen are associated with increased risk of severe ROP[11], the data from these reports suggest that $VEGF_{164}$ may be the splice variant most associated with pathologic features in ROP. VEGFR2 is believed to be the receptor most involved in angiogenic processes, whereas VEGFR1 is believed to trap VEGF and limit its signaling through VEGFR2 in development. Our data show VEGFR2, but not VEGFR1, as significantly upregulated in association with the ROP model.

We also found that VEGF protein concentration was significantly greater in the ROP model than room air at p14 when avascular retina existed in the ROP model, but vascularization of the inner retinal plexus had extended to the ora serrata in room air. These findings were

unexpected and contrast with other models of oxygen-induced retinopathy[5] in which VEGF expression was reduced following hyperoxia-induced avascular retina, and increased with relative hypoxia-induced endothelial cell proliferation into the vitreous[12,13]. The early concept of hyperoxia induced “vaso-obliteration” is clinically not observed in zone II, stage 3 severe ROP. Rather, there appears to be incomplete vascular development associated with preterm birth followed by a delay in peripheral retinal vascularization and then abnormal angiogenic patterning and proliferation at the junction of vascular and avascular retina. We did find that VEGF was significantly increased in the ROP model when IVNV occurred. However, using the ROP model, our findings do not fit the biphasic hypothesis in that we found increased VEGF in association with both avascular retina and IVNV.

Previously using the ROP model, increased VEGF-VEGFR2 signaling was found associated with first arteriolar tortuosity and venous dilation, similar in appearance to human plus disease, followed by IVNV, and both were reduced by inhibiting the bioactivity of VEGF with an intravitreous injection of a neutralizing antibody to VEGF[28,35]. Since VEGF is an angiogenic agonist, both IVNV and intraretinal vascularization would be anticipated to be reduced by an agent to inhibit VEGF bioactivity or signaling. However, neither a neutralizing antibody to VEGF[28] nor a VEGFR2 tyrosine kinase inhibitor[27] were found to interfere with ongoing intraretinal vascularization in the ROP model even though each intervention significantly reduced IVNV. Also, in a series of human infants with mostly zone II, stage 3 severe ROP, single injections of intravitreous bevacizumab were reported to cause regression of stage 3 ROP and permit ongoing retinal vascularization toward the ora serrata[36]. These studies along with our data suggest that excessive VEGF-VEGFR2 expression and/or signaling are associated with IVNV and greater avascular retinal area in the ROP model and in some cases of severe human ROP. Further study is warranted.

The processes of developmental and aberrant angiogenesis are complex, involving a number of interacting factors. However, VEGF has been recognized as one of the most important in human retinal diseases associated with pathologic angiogenesis.[37,38] VEGF is upregulated by hypoxia and ischemia[34] and is increased in the serum and vitreous of patients with intravitreous neovascularization, including ROP[39,17]. Also, in a human infant with stage 3 ROP, VEGF mRNA was detected in the avascular retina[40]. Other pathways, including the delta-like ligand 4/Notch1 signaling pathway, can regulate the numbers of VEGF-induced endothelial tip cells to stalk cells at the junction of vascular and avascular retina and permit developmental angiogenesis[41,42]. Other angiogenic factors including erythropoietin, IGF-1, tumor necrosis factor, and hypoxia inducible factor-1α (HIF-1α), angiopoietins, tumor necrosis factor alpha, hepatocyte growth factor[43,20,44,45] have been reported to play a role in oxygen-induced retinopathy. Inhibitors, such as thrombospondin-1[46] and PEDF[47], may also be important. Interactions of growth factors and of other cells, such as pericytes, astrocytes and other glia[48,49] are important. Signaling events can affect endothelial tip cell filopodia number and length at the migrating front[27] and affect the patterning of vessels[50].

Direct comparisons between mathematical fold changes in expression of mRNAs with biologic outcomes fail to take into account signaling cascades. Variability in measurements can also occur within the oxygen cycle and reflect the time for protein translation, post-translational modification of protein, stability of mRNA, and sequestration of growth factor within extracellular matrix following mRNA upregulation. For the receptors, commercially available antibodies that recognize rat have not produced consistent results. Future studies of receptor protein and signaling will be important. Despite limitations, these data are useful to refine hypotheses on features of severe ROP seen today.

$VEGF_{188}$ mRNA was expressed in room air to a greater degree than in retinas from the ROP model. This splice variant is cell-associated, and its expression may reflect the vascular

coverage of the retina. There was also upregulation following hypoxia, a finding we had reported previously with relative quantitative RT-PCR[33]. However, there were no significant statistical associations between $VEGF_{188}$ and either developmental age or exposure to the ROP model.

In conclusion, we used a model that represents zone II, stage 3 severe ROP as observed in countries like the US where oxygen regulation and monitoring are implemented in neonatal intensive care units. We found that the expressions of splice variant $VEGF_{164}$ and VEGFR2 were significantly increased in association with older developmental age and exposure to the ROP model compared to room air, whereas $VEGF_{120}$ and VEGFR1 were increased in association with older developmental age. The fold change of $VEGF_{164}$ expression and the concentration of VEGF protein were greater in the ROP model at p14 when there was about 30 percent avascular retina compared to room air when the inner vascular plexus had extended to the ora serrata. Additional studies are needed to explore the association of increased VEGF with avascular retina.

Although this study supports others in the literature that excessive VEGF signaling is involved in the pathology of zone II, stage 3 severe ROP, the following considerations should be made before using anti-VEGF agents in the preterm infant eye. Inhibiting VEGF bioactivity in the preterm infant undergoing retinal and neurologic development may have adverse consequences, because VEGF is both a neuronal and endothelial survival factor[51,52,53]. Also, the development of the lung[54] requires VEGF and preterm infants are at risk for pulmonary disease. In addition, circulating drug levels are likely to be higher in infants than adults, because infants have relatively much smaller blood volumes than adults compared to the differences between respective vitreous volumes[23]. This study describes a model of zone II, stage 3 ROP and may not be relevant to other severe forms of ROP, such as aggressive posterior ROP. Finally, the Early Treatment Retinopathy of Prematurity Trial reported that laser treatment of type 1 prethreshold ROP was associated with 90% success[55]. Therefore, clinical trials are needed to test agents against the current standard of care.

Acknowledgments

Supported by NEI/NIH: EY015130, EY017011, March of Dimes, American Diabetes Association, Research to Prevent Blindness Physician Scientist Award (MEH).

MEH is a consultant for Ophthalmic Research Associates, Andover, MA for clinical trial development, not involved in this study.

MEH is the Principal Investigator and Corresponding Author and has had full access to all the data in the study and takes responsibility for the integrity of the data and the accuracy of the data analysis.

References

1. Terry TL. Extreme prematurity and fibroblastic overgrowth of persistent vascular sheath behind each crystalline lens:(1) Preliminary report. Am J Ophthalmol. 1942; 25:203–204.
2. Ashton N, Ward B, Serpell G. Effect of oxygen on developing retinal vessels with particular reference to the problem of retrolental fibroplasia. Br J Ophthalmol. 1954; 38:397–430. [PubMed: 13172417]
3. Patz A, Eastham A, Higginbotham DH, Kleh T. Oxygen studies in retrolental fibroplasia. Am J Ophthalmol. 1953; 36:1511–1522. [PubMed: 13104558]
4. Michaelson IC. The mode of development of the vascular system of the retina. With some observations on its significance for certain retinal diseases. Trans Ophthal Soc UK. 1948; 68:137–180.
5. Smith LEH, Wesolowski E, McLellan A, et al. Oxygen induced retinopathy in the mouse. Invest Ophthalmol Vis Sci. 1994; 35:101–111. [PubMed: 7507904]

6. Stiller R, Mering Rv, König V, Huch A, Huch R. How well does reflectance pulse oximetry reflect intrapartum fetal acidosis? Am J Obstet Gynecol. 2002; 186:1351–1357. [PubMed: 12066121]
7. Smith LE. Through the Eyes of a Child: Understanding Retinopathy through ROP. The Friedenwald Lecture. Invest Ophthalmol Vis Sci. 2008
8. Hellstrom A, Engstrom E, Hard A-L, et al. Postnatal serum insulin-like growth factor I deficiency is associated with retinopathy of prematurity and other complications of premature birth. Pediatrics. 2003; 112:1016–1020. [PubMed: 14595040]
9. Hellstrom A, Hard AL, Engstrom E, et al. Early Weight Gain Predicts Retinopathy in Preterm Infants: New, Simple, Efficient Approach to Screening. Pediatrics. 2009; 123:e638–e645. [PubMed: 19289449]
10. Penn JS, Henry MM, Wall PT, Tolman BL. The range of PaO2 variation determines the severity of oxygen induced retinopathy in newborn rats. Invest Ophthalmol Vis Sci. 1995; 36:2063–2070. [PubMed: 7657545]
11. Cunningham S, Fleck BW, Elton RA, Mclntosh N. Transcutaneous oxygen levels in retinopathy of prematurity. Lancet. 1995; 346:1464–1465. [PubMed: 7490994]
12. Pierce E, Foley E, Lois EH. Regulation of vascular endothelial growth factor by oxygen in a model of retinopathy of prematurity. Arch Ophthalmol. 1996; 114:1219–1228. [PubMed: 8859081]
13. Gao G, Li Y, Zhang D, et al. Unbalanced expression of VEGF and PEDF in ischemia-induced retinal neovascularization. FEBS Lett. 2001; 489:270–276. [PubMed: 11165263]
14. Carmeliet P, Ferreira V, Breier G, et al. Abnormal blood vessel development and lethality in embryos lacking a single VEGF allele. Nature. 1996; 380:435–439. [PubMed: 8602241]
15. Chan-Ling T, Gock B, Stone J. The effect of oxygen on vasoformative cell division: Evidence that 'physiological hypoxia' is the stimulus for normal retinal vasculogenesis. Invest Ophthalmol Vis Sci. 1995; 36:1201–1214. [PubMed: 7775098]
16. Stone J, Itin A, Alon T, et al. Development of retinal vasculature is mediated by hypoxia-induced vascular endothelial growth factor (VEGF) expression by neuroglia. J Neurosci. 1995; 15:4738–4747. [PubMed: 7623107]
17. Sonmez K, Drenser KA, Capone A Jr, Trese MT. Vitreous Levels of Stromal Cell-Derived Factor 1 and Vascular Endothelial Growth Factor in Patients with Retinopathy of Prematurity. Ophthalmology. 2008; 115:1065–1070. [PubMed: 18031819]
18. Alon T, Hemo I, Itin A, et al. Vascular endothelial growth factor acts as a survival factor for newly formed retinal vessels and has implications for retinopathy of prematurity. Nat Med. 1995; 1:1024–1028. [PubMed: 7489357]
19. Lofqvist C, Chen J, Connor KM, et al. From the Cover: IGFBP3 suppresses retinopathy through suppression of oxygen-induced vessel loss and promotion of vascular regrowth. PNAS. 2007; 104:10589–10594. [PubMed: 17567756]
20. Hellstrom A, Peruzzu C, Ju M, et al. Low IGF-1 suppresses VEGF-survival signalling in retinal endothelial cells: direct correlation with clinical retinopathy of prematurity. Proc Natl Acad Sci USA. 2001; 98:5804–5808. [PubMed: 11331770]
21. Chang KH, Chan-Ling T, McFarland EL, et al. IGF binding protein-3 regulates hematopoietic stem cell and endothelial precursor cell function during vascular development. PNAS. 2007; 104:10595–10600. [PubMed: 17567755]
22. Penn JS, Henry MM, Tolman BL. Exposure to alternating hypoxia and hyperoxia causes severe proliferative retinopathy in the newborn rat. Pediatr Res. 1994; 36:724–731. [PubMed: 7898981]
23. Hartnett ME, Martiniuk DJ, Saito Y, et al. Triamcinolone Reduces Neovascularization, Capillary Density and IGF-1 Receptor Phosphorylation in a Model of Oxygen-Induced Retinopathy. Investigative Ophthalmology Visual Science. 2006; 47:4975–4982. [PubMed: 17065516]
24. Liu K, Akula JD, Falk C, Hansen RM, Fulton AB. The Retinal Vasculature and Function of the Neural Retina in a Rat Model of Retinopathy of Prematurity. Investigative Ophthalmology Visual Science. 2006; 47:2639–2647. [PubMed: 16723481]
25. Penn JS, Tolman BL, Henry MM. Oxygen-induced retinopathy in the rat: Relationship of retinal nonperfusion to subsequent neovascularization. Invest Ophthalmol Vis Sci. 1994; 35:3429–3435. [PubMed: 8056518]

26. Chan-Ling T. Glial, vascular and neuronal cytogenesis in whole-mounted cat retina. Microsc Res Tech. 1997; 36:1–16. [PubMed: 9031257]
27. Budd S, Byfield G, Martiniuk D, Geisen P, Hartnett ME. Reduction in endothelial tip cell filopodia corresponds to reduced intravitreous but not intraretinal vascularization in a model of ROP. Exp Eye Res. 2009 in press.
28. Geisen P, Peterson L, Martiniuk D, Uppal A, Saito Y, Hartnett ME. Neutralizing antibody to VEGF reduces intravitreous neovascularization and does not interfere with vascularization of avascular retina in an ROP model. Mol Vis. 2008; 14:345–357. [PubMed: 18334951]
29. Werdich XQ, Penn JS. Specific Involvement of Src Family Kinase Activation in the Pathogenesis of Retinal Neovascularization. Investigative Ophthalmology Visual Science. 2006; 47:5047–5056. [PubMed: 17065526]
30. Lowry OH, Rosebrough NJ, Farr AL, Randall RJ. Protein measurement with the folin phenol reagent. J Biol Chem. 1951; 193:265–275. [PubMed: 14907713]
31. Vandesompele J, De Preter K, Pattyn F, et al. Accurate normalization of real-time quantitative RT-PCR data by geometric averaging of multiple internal control genes. Genome Biol. 2002; 3:0034.1–0034.12.
32. Edwards D, Berry JJ. The efficiency of simulation-based multiple comparisons. Biometrics. 1987; 43:913–928. [PubMed: 3427176]
33. McColm JR, Geisen P, Hartnett ME. VEGF isoforms and their expression after a single episode of hypoxia or repeated fluctuations between hyperoxia and hypoxia: Relevance to clinical ROP. Mol Vis. 2004; 10:512–520. [PubMed: 15303088]
34. Ferrara N, Gerber HP, Lecouter J. The biology of VEGF and its receptors. Nat Med. 2003; 9:669–676. [PubMed: 12778165]
35. Hartnett ME, Martiniuk DJ, Byfield GE, Geisen P, Zeng G, Bautch VL. Neutralizing VEGF decreases tortuosity and alters endothelial cell division orientation in arterioles and veins in rat model of ROP: Relevance to plus disease. Invest Ophthalmol Vis Sci. 2008 Mar 31. epub: 7-3107.
36. Mintz-Hittner HA, Kuffel RR Jr. Intravitreal injection of bevacizumab (avastin) for treatment of stage 3 retinopathy of prematurity in zone I or posterior zone II. Retina. 2008; 28:831–838. [PubMed: 18536599]
37. Robinson GS, Aiello LP. Angiogenic factors in diabetic ocular disease: Mechanisms of today, therapies for tomorrow. International Ophthalmology Clinics. 1998; 38:89–102. [PubMed: 9604739]
38. Adamis AP, Miller JW, Bernal MT, et al. Increased vascular endothelial growth factor levels in the vitreous of eyes with proliferative diabetic retinopathy. Am J Ophthalmol. 1994; 118:445–450. [PubMed: 7943121]
39. Aiello LP, Avery RL, Arrigg PG, et al. Vascular endothelial growth factor in ocular fluid of patients with diabetic retinopathy and other retinal disorders. New Eng J Med. 1994; 331:1480–1487. [PubMed: 7526212]
40. Young TL, Anthony DC, Pierce E, Foley E, Smith LEH. 1Histopathology and vascular endothelial growth factor in untreated and diode laser-treated retinopathy of prematurity. JAAPOS. 1997; 1:105–110.
41. Hellstrom M, Phng LK, Hofmann JJ, et al. Dll4 signalling through Notch1 regulates formation of tip cells during angiogenesis. Nature. 2007; 445:776–780. [PubMed: 17259973]
42. Bentley K, Gerhardt H, Bates PA. Agent-based simulation of notch-mediated tip cell selection in angiogenic sprout initialisation. Journal of Theoretical Biology. 2008; 250:25–36. [PubMed: 18028963]
43. Smith LEH, Kopchick JJ, Chen W, et al. Essential role of growth hormone in ischemia-induced retinal neovascularization. Science. 1997; 276:1706–1709. [PubMed: 9180082]
44. Morita M, Ohneda O, Yamashita T, et al. HLF/HIF-2alpha is a key factor in retinopathy of prematurity in association with erythropoietin. EMBO J. 2003; 22:1134–1146. [PubMed: 12606578]
45. Smith LEH, Shen W, Peruzzu C, et al. Regulation of vascular endothelial growth factor-dependent retinal neovascularization by insulin-like growth factor-1 receptor. Nat Med. 1999; 5:1390–1395. [PubMed: 10581081]

46. Wu Z, Wang S, Sorenson CM, Sheibani N. Attenuation of retinal vascular development and neovascularization in transgenic mice over-expressing thrombospondin-1 in the lens. Dev Dyn 2006. 2006; 235:1908–1920.
47. Dawson DW, Volpert OV, Gillis P, et al. Pigment epithelium-derived factor: a potent inhibitor of angiogenesis. Science. 1999; 285:245–248. [PubMed: 10398599]
48. Huang Q, Wang S, Sorenson CM, Sheibani N. PEDF-deficient mice exhibit an enhanced rate of retinal vascular expansion and are more sensitive to hyperoxia-mediated vessel obliteration. Exp Eye Res. 2008; 87:226–241. [PubMed: 18602915]
49. Dorrell MI, Aguilar E, Jacobson R, et al. Maintaining retinal astrocytes normalizes revascularization and prevents vascular pathology associated with oxygen-induced retinopathy. Glia. 2009 in press.
50. Shibuya M. Differential Roles of Vascular Endothelial Growth Factor Receptor-1 and Receptor-2 in Angiogenesis. j Biochem Molecul Biol. 2006; 39:469–478.
51. Oosthuyse B, Moons L, Storkebaum E, et al. Deletion of the hypoxia-response element in the vascular endothelial growth factor promoter causes motor neuron degeneration. Nat Genet. 2001; 28:131–138. [PubMed: 11381259]
52. Laudenbach V, Fontaine RH, Medja F, et al. Neonatal hypoxic preconditioning involves vascular endothelial growth factor. Neurobiology of Disease. 2007; 26:243–252. [PubMed: 17306552]
53. Nishijima K, Ng YS, Zhong L, et al. Vascular Endothelial Growth Factor-A Is a Survival Factor for Retinal Neurons and a Critical Neuroprotectant during the Adaptive Response to Ischemic Injury. Am J Path. 2007; 171:53–67. [PubMed: 17591953]
54. Voelkel NF, Vandivier RW, Tuder RM. Vascular endothelial growth factor in the lung. Am J Physiol Lung Cell Mol Physiol. 2006; 290:L209–L221. [PubMed: 16403941]
55. Early Treatment for Retinopathy of Prematurity Cooperative Group. Revised Indications for the Treatment of Retinopathy of Prematurity: Results of the Early Treatment for Retinopathy of Prematurity Randomized Trial. Arch Ophthalmol. 2003; 121:1684–1694. [PubMed: 14662586]

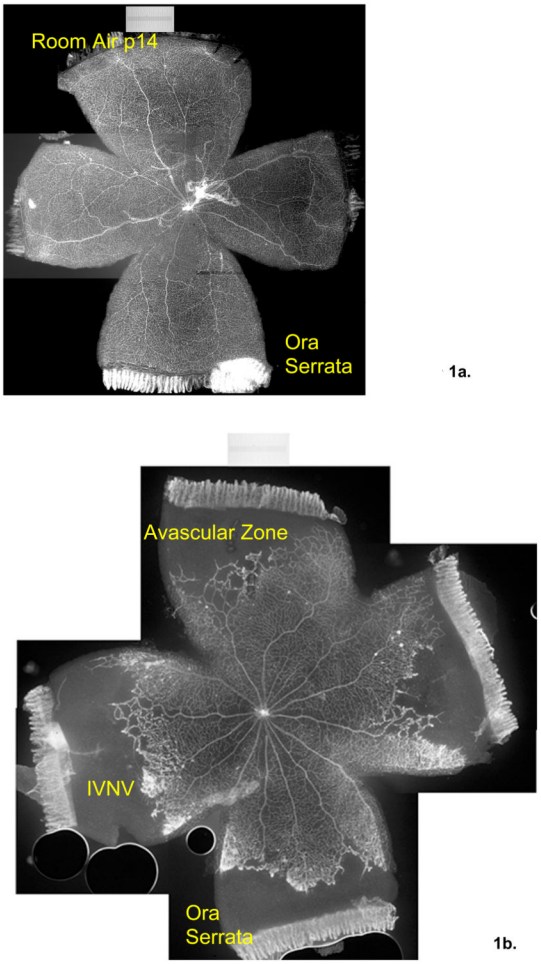

Figure 1.

Lectin-stained retinal flat mounts created by 4 relaxing incisions showing retinal vascularization in rat. A). Room air raised pup at postnatal day (p)14 rat has retinal vascularization that extends to the ora serrata.

B) ROP model at p18 following 7 cycles of oxygen fluctuations between 50% and 10% and then 4 days in room air, showing avascular retina and intravitreous neovascularization (IVNV). Optic nerve is in the center (no macula is present in rat) and peripheral avascular retina seen adjacent to the ora serrata.

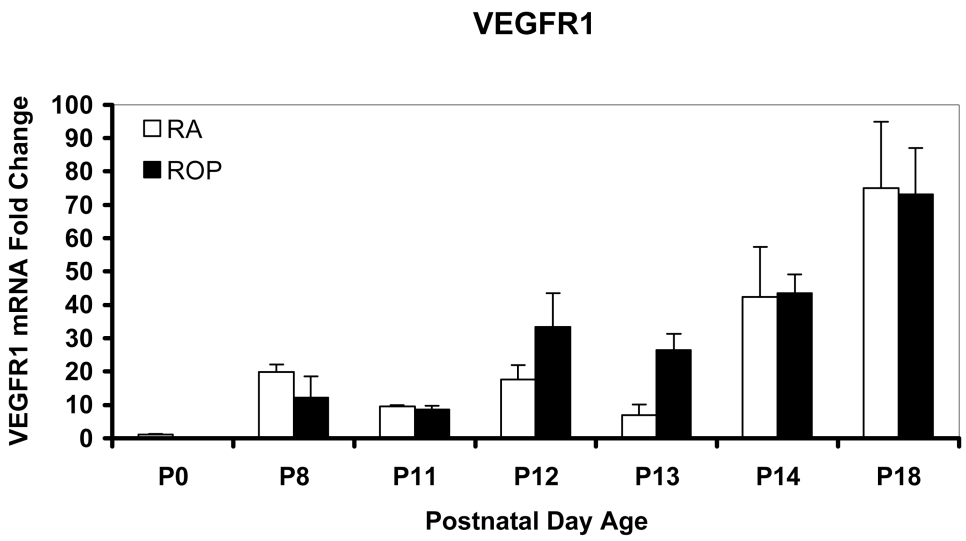

Figure 2.

Real time PCR mean values for VEGF Receptor (R)1 of rat pups from p0 through p18 in room air development (RA) or in the ROP model (ROP). In the ROP model, p8, p12, and p14 occur immediately following hypoxia (10% FiO_2) and p11 and p13 following hyperoxia (50% FiO_2). Following p14, pups are in room air (21% FiO_2). All values are normalized to β-actin and are compared to p0, which is the same for room air and ROP. There was a significant increase in expression associated with older developmental age (P<.0001) but not with exposure to the ROP model compared to age-matched room air pups (P=.82). The value for VEGFR1 at p0 was scaled to 1.0 to allow comparisons among VEGFR1 values in room air or ROP. The graph represents means and standard errors for each room air and ROP time point, each time point having an n=at least 5 retinas from different pups taken from at least 2 litters.

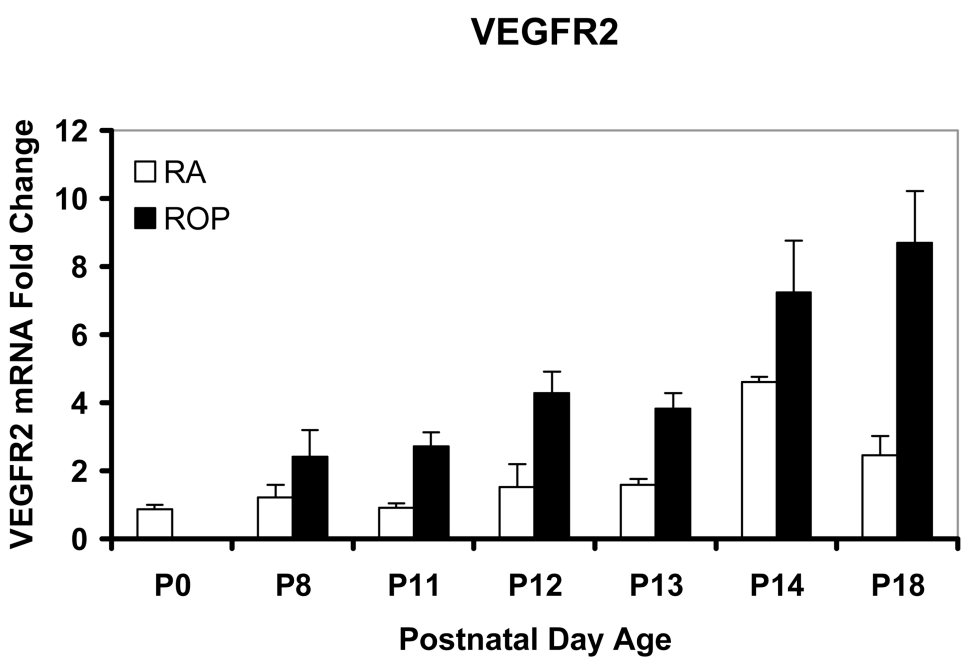

Figure 3.

Real time PCR mean values for VEGF Receptor (R)2 of rat pups from p0 through p18 in room air development (RA) or in the ROP model (ROP). In the ROP model, p8, p12, and p14 occur immediately following hypoxia (10% FiO_2) and p11 and p13 following hyperoxia (50% FiO_2). Following p14, pups are in room air (21% FiO_2). All values are normalized to β-actin and are compared to p0 which is the same for room air and OIR. There was a significant increase in VEGFR2 expression associated with older developmental age (*P*<. 0001) and with exposure to the ROP model compared to age-matched room air pups (*P*=. 0247). The value for VEGFR2 at p0 was scaled to 1.0 to allow comparison among VEGFR2 values in room air or ROP. The graph represents means and standard errors for each room air and ROP time point, each time point having an n=at least 5 retinas from different pups taken from at least 2 litters.

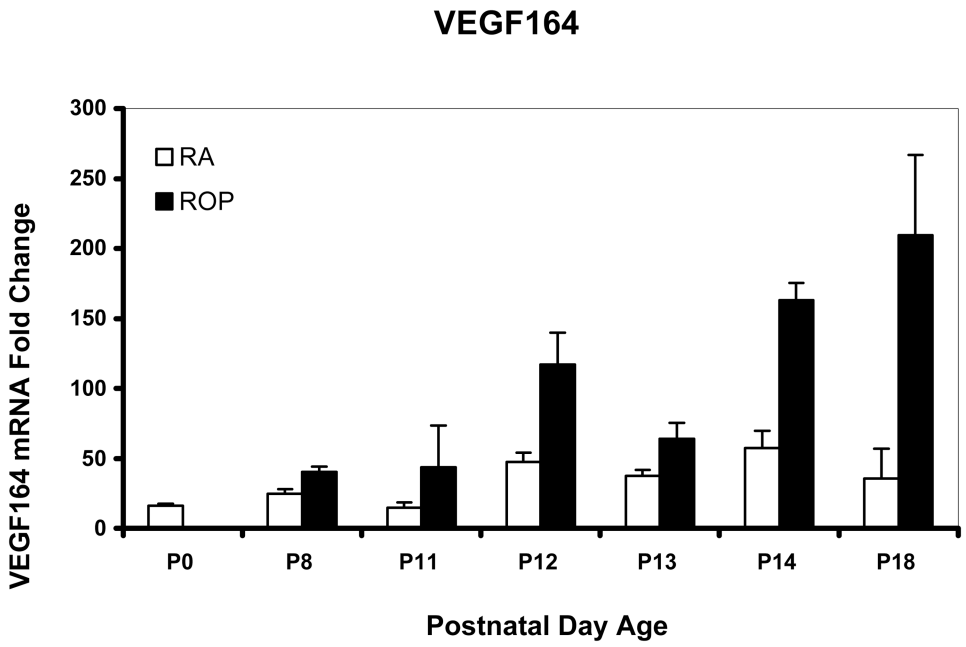

Figure 4.

Real time PCR mean values for VEGF splice variant $VEGF_{164}$ of rat pups from selected postnatal days (p) 0 through p18 in room air development (RA) or in the ROP model (ROP). In the ROP model, p8, p12, and p14 occur immediately following hypoxia (10% FiO_2) and p11 and p13 following hyperoxia (50% FiO_2). Following p14, pups are in room air (21% FiO_2). At p14, in room air the inner retina is vascularized to the ora serrata, whereas in the ROP model, there is 30% avascular retina. All values are normalized to β-actin and are compared to p0 which is the same for room air and OIR. There was a significant increase in expression associated with older developmental age (P<.0001) and with exposure to the ROP model compared to age-matched room air pups (P<.0001). For graphical representations, the value of $VEGF_{188}$ mRNA at p0 was scaled to 1.0 and fold expression of mRNAs of the splice variants at time points in RA and the ROP model were related to it. The graph represents means and standard errors for each room air and ROP time point, each time point having an n=at least 5 retinas from different pups taken from at least 2 litters.

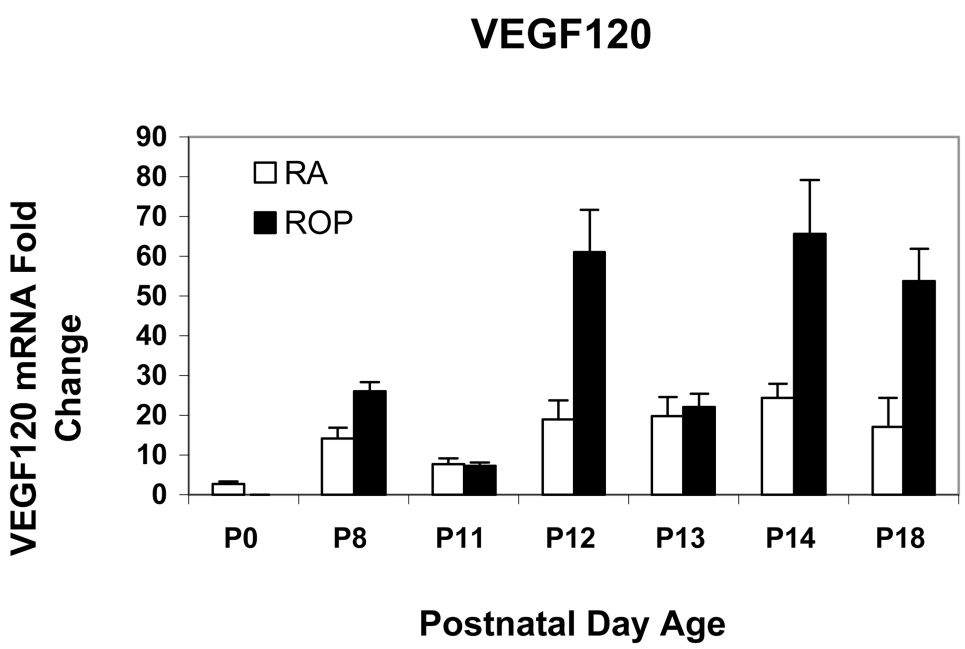

Figure 5.

Real time PCR mean values for VEGF splice variant $VEGF_{120}$ of rat pups from selected postnatal days (p) 0 through p18 in room air development (RA) or in the ROP model (ROP). In the ROP model, p8, p12, and p14 occur immediately following hypoxia (10% FiO_2) and p11 and p13 following hyperoxia (50% FiO_2). Following p14, pups are in room air (21% FiO_2). At p14, in room air the inner retina is vascularized to the ora serrata, whereas in the ROP model, there is 30% avascular retina. All values are normalized to β-actin and are compared to p0 which is the same for room air and OIR. There was a significant increase in expression associated with older developmental age ($P<.0001$) but not with exposure to the ROP model compared to age-matched room air pups ($P=.614$). For graphical representations, the value of $VEGF_{188}$ mRNA at p0 was scaled to 1.0 and fold expression of mRNAs of the splice variants at time points in RA and the ROP model were related to it. The graph represents means and standard errors for each room air and ROP time point, each time point having an n=at least 5 retinas from different pups taken from at least 2 litters.

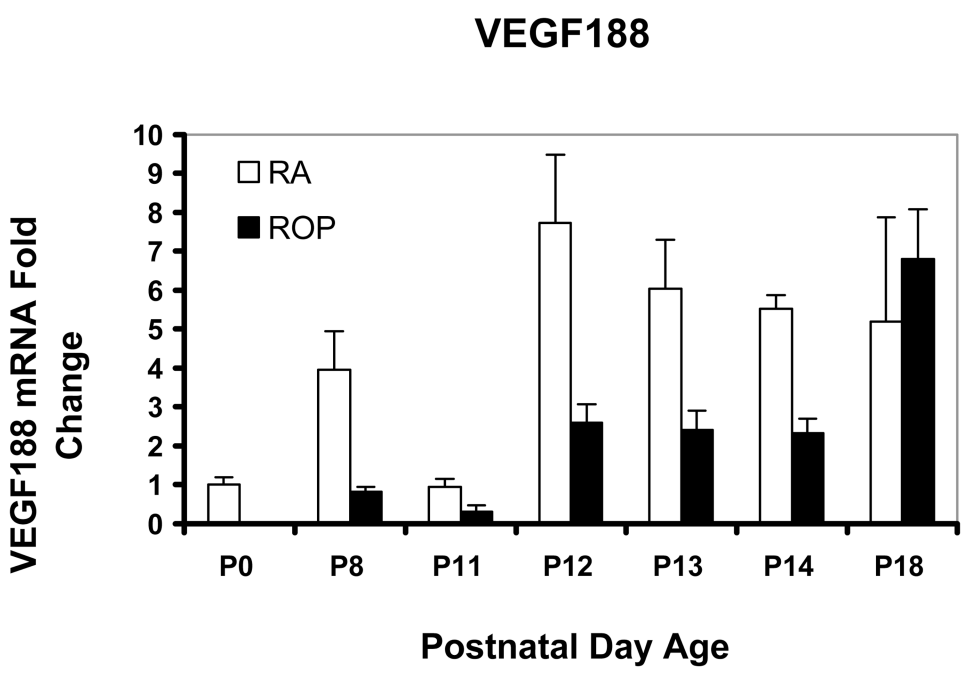

Figure 6.

Real time PCR mean values for VEGF splice variant $VEGF_{188}$ of rat pups from selected postnatal days (p) 0 through p18 in room air development (RA) or in the ROP model (ROP). In the ROP model, p8, p12, and p14 occur immediately following hypoxia (10% FiO_2) and p11 and p13 following hyperoxia (50% FiO_2). Following p14, pups are in room air (21% FiO_2). At p14, in room air the inner retina is vascularized to the ora serrata, whereas in the ROP model, there is 30% avascular retina. All values are normalized to β-actin and are compared to p0 which is the same for room air and OIR. There was no significant association with older developmental age or with exposure to the ROP model compared to age-matched room air pups. For graphical representations, the value of $VEGF_{188}$ mRNA at p0 was scaled to 1.0 and fold expression of mRNAs of the splice variants at time points in RA and the ROP model were related to it. The graph represents means and standard errors for each room air and ROP time point, each time point having an n=at least 5 retinas from different pups taken from at least 2 litters.

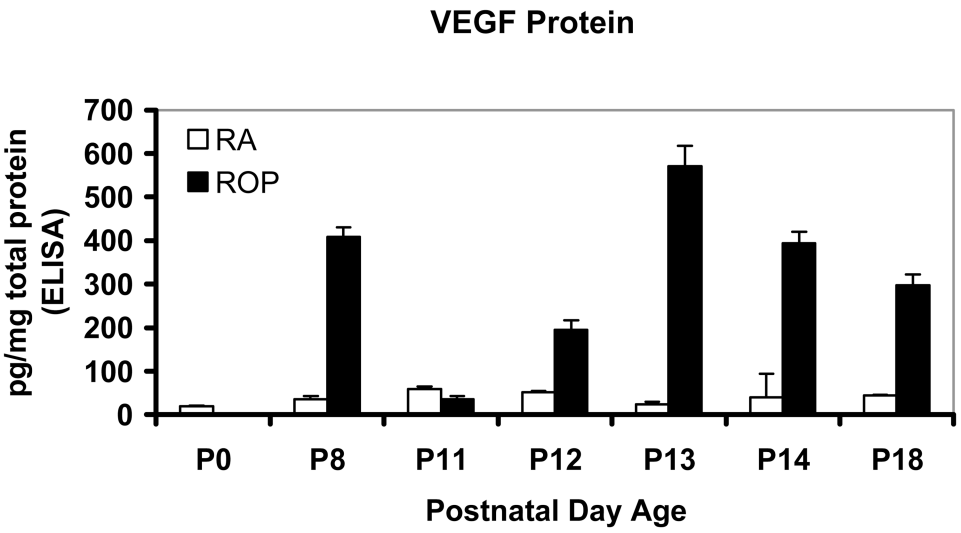

Figure 7.

ELISA measurements of retinal VEGF at time points in room air development (RA) or ROP model (ROP). There was a significant increase in expression associated with older developmental age ($P<.0001$) and with exposure to the ROP model compared to age-matched room air pups ($P<.0001$). In Post-hoc testing, VEGF was significantly increased in the ROP model compared to room air at p14 and p18 ($P<.0001$). For each time point, an n= at least 5 retinas from different pups were analyzed from at least 2 different litters.